

Design and Performance Evaluation of Metamaterial-Based Triple-Band Rectangular Microstrip Antenna for Wireless Communications

Udoh Mary Lambert¹; Udofia Kufre Michael²
Department of Electrical and Electronics Engineering,
University of Uyo, Uyo

Saturday Chukwudi Jeffrey³
Department of Electrical and Electronics Engineering,
Joseph Sarwuan Tarka University, Markudi

Abstract:- Numerous writers have hinted at the necessity for broader bandwidth coverage of microwave frequency communication employing tiny antennas, and various solutions have been put forth. This study presents a metamaterial-based microstrip triple band antenna with operating frequencies of 2.4 GHz, 3.5 GHz, and 5 GHz proposed for X-band fifth generation (5G) application. A metamaterial-based microstrip antenna with integrated square complementary split ring resonators (CSRR) was designed, simulated, and analyzed. The design of microstrip patch was done using transmission line equations, and analysis was done using full wave model with the aid of Computer Simulation Technology (CST) Studio software. Flame Resistant (FR-4) substrate with a dielectric constant of 4.2 and thickness of 1.6 mm was chosen mainly for maintaining compact antenna geometry. Bandwidths of 820 MHz, 1600 MHz, and 800 MHz were achieved at 2.4 GHz, 3.5 GHz, and 6 GHz by the proposed metamaterial-based antenna. The proposed antenna also showed good potential as it resonated equally at higher frequencies beyond 12.7 GHz, broadening its application horizon. Regarding the proposed antenna's bandwidth performance, it is recommended to be utilized for devices that are not as compact yet require a wide range of frequency coverage.

Keywords:- Bandwidth, metamaterial, microstrip antenna, fifth generation, triple band.

I. INTRODUCTION

The modern drive for increased data speed, spectral efficiency, near-zero latency, and better connectivity has spurred many communications standard developments [1]. According to Yost [2], the introduction of long-term evolution (LTE) of mobile communication was aimed at the continuous advancement of wireless broadband technology that birthed the fifth generation of wireless communication (popularly known as 5G) with higher data throughput, ultra-low latency, massive network capacity, millimeter wave (mm-Wave) carrier aggregation (CA), and higher overall reliability than the previous generations. To accommodate the complexity of 5G subsystems, especially during deployment, advanced antenna systems (AAS) with multi-antenna techniques like beamforming and massive multiple-input and multiple-output (mMIMO) are combined [3], [4].

Microstrip antenna (MSA) topologies provide a feasible solution to make up for propagation-related problems caused by 5G pathloss for short-range communications, according to [5]. To enhance the bandwidth characteristics of MSAs, metamaterials (MTM) such as split ring resonators (SRR) are integrated into their geometries [6]–[8]. The dual electromagnetic behavior of SRR facilitates modification of antenna parameters (using single negative or double negative MTM). SRRs are described by [9] as artificial materials with the innate potential to display electromagnetic features not typically found in naturally existing material, like artificial magnetism and negative refractive index.

This study proposes a tripartite band double negative metamaterial-based rectangular microstrip antenna (RMSA) for wireless communication, along with an assessment of its performance. The frequencies of concern are the Industrial Scientific and Medical (ISM) band, the 5 GHz bands, and the frequency that Nigeria is allowed to implement 5G.

II. REVIEW OF RELATED LITERATURES

Triple-band L-dumbbell-shaped antenna for Worldwide Interoperability for Microwave Access (WiMAX) and Wireless Local Area Networks (WLAN) designed and analyzed using finite difference time domain (FDTD) was presented by [7]. The antenna consisted of two L-dumbbell-shaped unit cells, a microstrip feed line, and a partial ground plane. Their proposed antenna showed tripled band features with impedance bandwidths of 10.6, 4.67, and 26.8% at resonating frequencies of 2.4, 3, and 5.7 GHz, respectively. The set objectives by the authors were achieved but the geometry adopted differs from any famous geometry of unit cell of metamaterial known to contribute to material reconfiguration toward obtaining either single negative or double negative metamaterial (SNG or DNG) characteristics.

Hamad et al. [10] presented the triple band metamaterial-based microstrip antenna design for WLAN and WiMAX (2.4/3.5/5.6 GHz) applications. The authors achieved triple band resonance by etching one rectangular and two circular split ring resonator (SRR) unit cells in opposite directions on an RT/Duroid 5880 substrate and ground plane of a standard patch operating at 3.56 GHz. The two circular cells were introduced to resonate at 5.3 GHz for the WiMAX band, while the rectangular cell was designed to resonate at 2.45 GHz for the WLAN band.

They also proposed the placement of a complementary H-shaped unit cell acting as lens positioned above the triple band antenna to increase antenna gain. However, despite the fits achieved by the authors, there was a consistent misrepresentation of the unit cell return loss in most of their plots; S_{11} was equated to S_{21} , which is an inaccurate interpretation of scattering parameters and affected the results of their prototype. The authors' plots would find better representation in measuring the mutual coupling of antennas.

A rectangular dielectric resonator antenna (DRA) for cognitive radio with two symmetrical short-circuited strips for enhanced isolation between two ports was proposed by Yongfeng [11]. The authors presented a compact UWB dielectric resonator antenna with dual-band-rejection characteristics for WiMAX/WLAN bands. By embedding stub and slot of different lengths on a DRA, they were able to increase bandwidth. A small bi-cone dielectric resonator antenna for ultra-wideband applications was also presented their report. However, the design of these DRA antennas imposed an inherent restriction on the scope of their use.

An obround-shaped metamaterial-based small planar antenna was described by [12] for use in UWB and 5G applications. The antenna was built on a Rogers RT Duroid 5880 substrate with a thickness of 0.43 mm, resulting in a fractional bandwidth of over 50% and good radiation efficiency. Saraswat and Kumar [13] suggested a 36 x 22 x 1.6 mm³ metamaterial-inspired multiband antenna for 5G sub-6 GHz New Radio (NR) frequency bands and wireless applications. This antenna attained a fractional impedance bandwidth of 47.20 percent. Even though both proposed antennas performed well, they failed to properly articulate their design principles, particularly regarding the metamaterial they used.

III. METHODOLOGY

The transmission line model equations from [14] were used to create a single-band microstrip antenna that resonates at 3.5 GHz. The rectangular patch structure functions as a resonator, therefore, its length and width are commonly chosen so that, for effective and enhanced radiation, $L_p < W_p < 2L_p$. The following is a list of the precise design equations for the rectangular microstrip patch.

- The width (W_p) of the microstrip patch antenna computed from (1).

$$W_p = \frac{c}{2f_r \sqrt{\frac{\epsilon_r + 1}{2}}} \tag{1}$$

- The effective dielectric constant (ϵ_{reff}) is obtained from (2).

$$\epsilon_{reff} = \frac{\epsilon_r + 1}{2} + \frac{\epsilon_r - 1}{2} \left[1 + 12 \left(\frac{h}{W_p} \right) \right]^{-1/2} \tag{2}$$

- The effective length L_{eff} of the patch can be derived from (3).

$$L_{eff} = \frac{c}{2f_r \sqrt{\epsilon_{reff}}} \tag{3}$$

Calculation of the ground plane dimensions (L_g and W_g): The use of infinite ground planes is a key premise of the transmission line model. For practical considerations, a limited ground plane is necessary, nevertheless. The size of the ground plane for both finite and infinite ground planes is greater than the patch dimensions by around six times the substrate thickness all round [5]. Consequently, the ground plane dimensions for this design are determined as follows:

$$L_g = L_p + 6h \tag{4}$$

$$W_g = W_p + 6h \tag{5}$$

Determination of the patch thickness (t): The metallic patch is selected to be very thin such that $t \ll \lambda_0$. Dielectric constant (ϵ_r) of 4.2 was used for the antenna design.

The inset-fed technique was used for the feedline to the patch, and the design equations were adopted from [15], [16]. The schematic diagram and table containing computed dimensions of the 3.5 GHz single band patch antenna are shown in Fig. 1 and Table 1, respectively, while the designed 3.5 GHz antenna in CST Studio is shown in Fig. 2.

A. Unit cell metamaterial

Depending on the structure and size of a unit cell, different corresponding values of permittivity (ϵ), permeability (μ), and resonant frequencies (f_r) can be obtained. For each unit cell type, the dimensions of the unit cell can be adjusted to satisfy the condition at resonant frequency (f_r) [9]. According to [17], unit cell size is approximately one-tenth of the operating wavelength (λ_{air}); that is, the retrieval of effective parameters from reflection and transmission data depends on the fact that the unit-cell dimension should be smaller than the operating wavelength in the media. Hence, taking one-tenth of the wavelength of the reference antenna (3.5 GHz antenna) to be the external length (L_m) of the metamaterial (MTM), the outer ring length of the MTM is computed to be 8.57 mm. The MTM shape of choice for this project is the split ring resonator (SRR) selected mainly for ease of design and analysis. Based on the report put forward by [18], every dimension of the double square SRR is duly accounted with a simplified relationship between the components typified in the equivalent circuit presented in Fig. 3 (b), such as capacitance (C), inductance (L) and f_r given in (6).

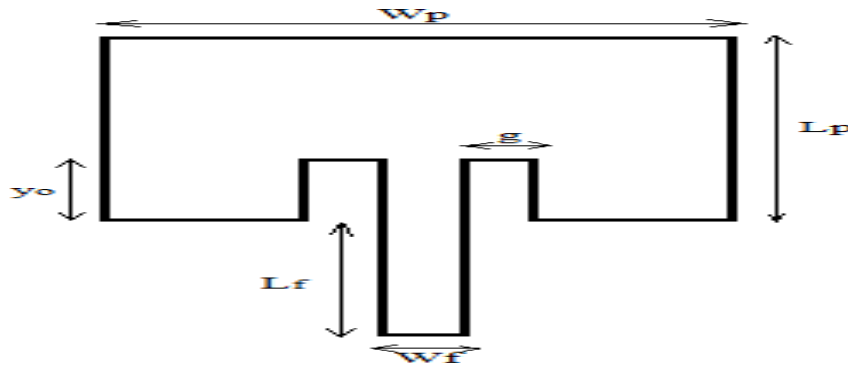


Fig. 1: Schematic diagram with dimensions of the designed antenna.

Table 1: Design dimensions of 3.5 GHz single band inset-fed RMSA

| Design Parameter | Values (mm) |
|---|-----------------|
| Patch dimensions: | |
| Length (L_p) | 20.45 |
| Width (W_p) | 26.58 |
| Substrate height (h) | 1.60 |
| Patch thickness (t) | 0.35 |
| Ground plane dimensions: | |
| Length of ground plane (L_g) | 30.05 |
| Width of ground plane (W_g) | 36.18 |
| Feed line dimensions: | |
| Width of 50 Ω transmission line (W_f) | 3.10 |
| Length of 50 Ω transmission line (L_f) | 4.80 |
| Input edge impedance of the patch (R_{in}) | 185.19 Ω |
| Feed line Characteristic impedance (Z_0) | 50 Ω |
| Inset fed gap (g) | 1.80 |
| Inset fed distance, (y_o) | 7.55 |

B. Unit Cell Metamaterial

Depending on the structure and size of a unit cell, different corresponding values of permittivity (ϵ), permeability (μ), and resonant frequencies (f_r) can be obtained. For each unit cell type, the dimensions of the unit cell can be adjusted to satisfy conditions at resonant frequency (f_r) [10]. According to [7], unit cell size is approximately one-tenth of the operating wavelength (λ_{air}); that is, the retrieval of effective parameters from reflection and transmission data depends on the fact that the unit-cell dimension should be smaller than the operating wavelength in the media. Hence, taking one-tenth of the wavelength of the reference antenna (3.5 GHz antenna) to be the external length (L_m) of the metamaterial (MTM),

the external ring length of the MTM is computed to be 8.57 mm. The MTM shape of choice for this project is the split ring resonator (SRR) selected mainly for ease of design and analysis. Based on the report put forward by [18], every dimension of the double square SRR is duly accounted with a simplified relationship between the components typified in the equivalent circuit presented in Fig. 3 (b), such as capacitance (C), inductance (L) and f_r given in (6).

$$L_m = \frac{85.71}{10} = 8.57 \text{ mm} \tag{6}$$

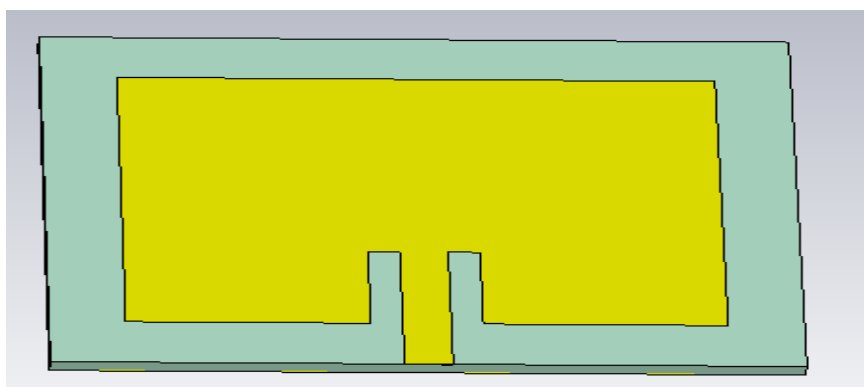


Fig. 2: Designed 3.5 GHz RMSA in CST Studio

The focus parameters are the ring's outer radius, a thickness, c, height, h, and the gap width, g. An inductance, L model the square SRR; the gap in the ring corresponds to capacitance, C_{gap} which is modelled as a parallel plate capacitor; the charges on the surface are the surface capacitance $C_{surface}$. According to [19], with a magnetic field applied along the z-axis, an electromotive force appears around the SRR, making the structure behave similarly to an L-C network with resonant frequency (f_r) expressed in (7).

$$f_r = \frac{1}{2\pi\sqrt{LC}} \tag{7}$$

Similarly, the inductance is approximated by a closed ring [19].

$$L = \mu_0 a_m \left(\ln \frac{8a_m}{h+c} - 0.5 \right) \tag{8}$$

Note: $a_m = a + \frac{w}{2}$

$$C_{gap} = \epsilon_0 \left(\frac{ch}{g} + \frac{2\pi h}{\ln \frac{2.4h}{c}} \right) \tag{9}$$

$$C_{surface} = \frac{2\epsilon_0 h}{\pi} \ln \frac{4a}{g} \tag{10}$$

$$\frac{1}{C} = \frac{1}{C_{gap}} + \frac{1}{C_{surface}} \tag{11}$$

where μ_0 is the permeability of free space, a is the outer radius of ring and a_m is the mean radius of the ring.

C. Patch Antenna with Metamaterial

The single band patch antenna designed at 3.5 GHz and SRR structure earlier simulated were integrated on an FR-4 substrate, and a partial ground plane was introduced to further offset current flow and alter the impedance bandwidth by shifting the antenna resonance frequency. This resulted in reduced patch antenna size at the same resonance frequency though with a modified antenna layout, as illustrated in Fig. 4. The augmented patch dimensions as well as that of SRR are given in Table II.

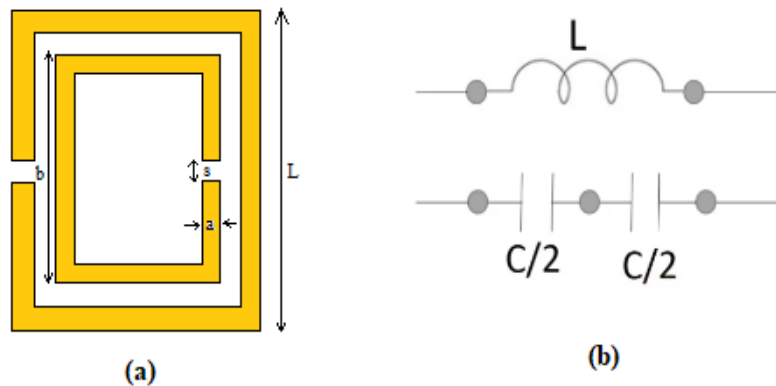


Fig. 3: Metamaterial (a) Geometry of unit cell SRR (b) Equivalent circuit representation of unit cell SRR [18]

IV. RESULTS AND DISCUSSION

The return loss of the single band patch antenna designed at a frequency of 3.5 GHz showing a minimum return loss value of -27.16 dB at 3.52 GHz, is presented in Fig. 5, while the S_{11} , and S_{21} plot of the metamaterial is

given in Figure 6, showing minimum return loss at 13.69 GHz at values of 22.49 and 60.47 dB. Real and imaginary plots of permittivity and permeability of the MTM is shown in Fig. 7 and Fig. 8.

Table 2: Dimensions of SRR AND proposed antenna

| Parameter | Value (mm) |
|-----------|------------|
| Lg | 25.00 |
| Wg | 30.00 |
| Lp | 13.00 |
| Wp | 14.00 |
| t | 0.035 |
| h | 1.60 |
| yo | 1.50 |
| g | 2.00 |
| L_r | 14.00 |
| W_r | 4.00 |
| L_m | 8.57 |
| s | 1.00 |
| a | 1.00 |
| b | 6.00 |

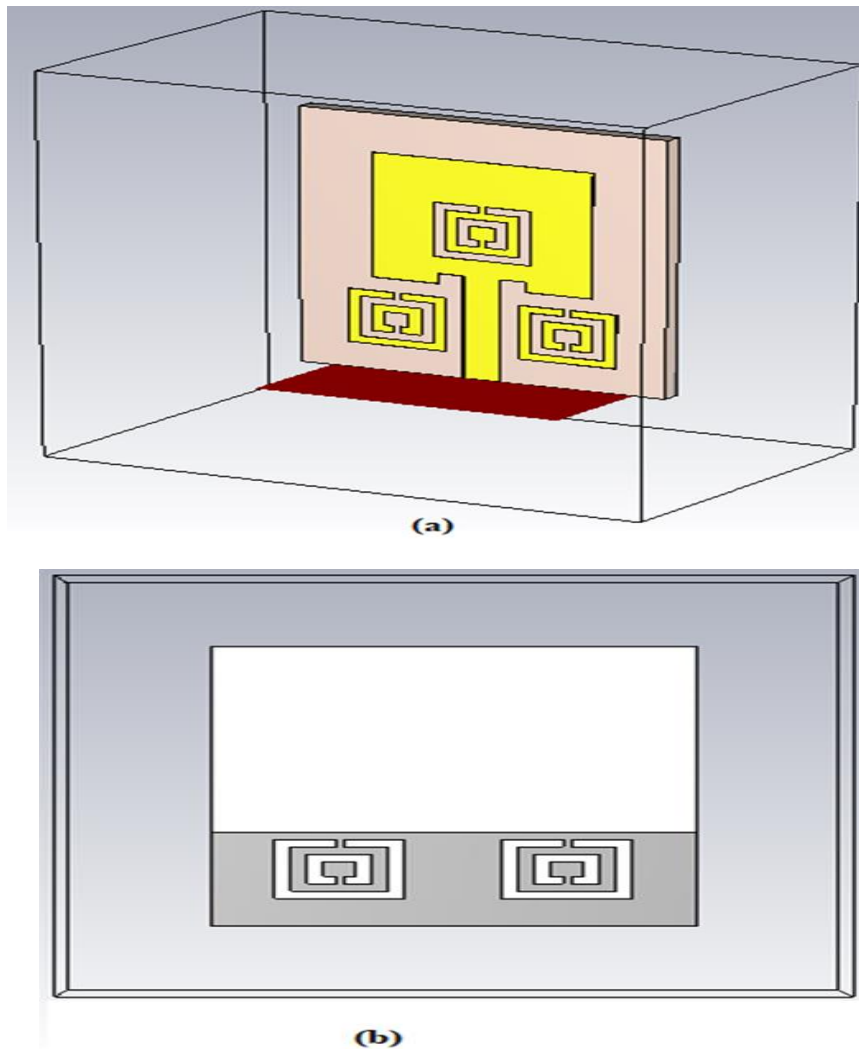


Fig. 4: Proposed MTM-based patch antenna in CST Studio (a) Front view (b) Back view

From Fig. 7 and Fig. 8, negative permittivity and permeability values at the resonance frequency of 11.95 GHz confirm the SRR adopted as a double negative (DU-negative) metamaterial. Fig. 9 gives the plot's return loss

plot of the proposed antenna from where a combined bandwidth of 8.66 GHz was obtained over two distinct frequencies of (3.4009 GHz – 11.721 GHz and 2.869 GHz – 3.211 GHz).

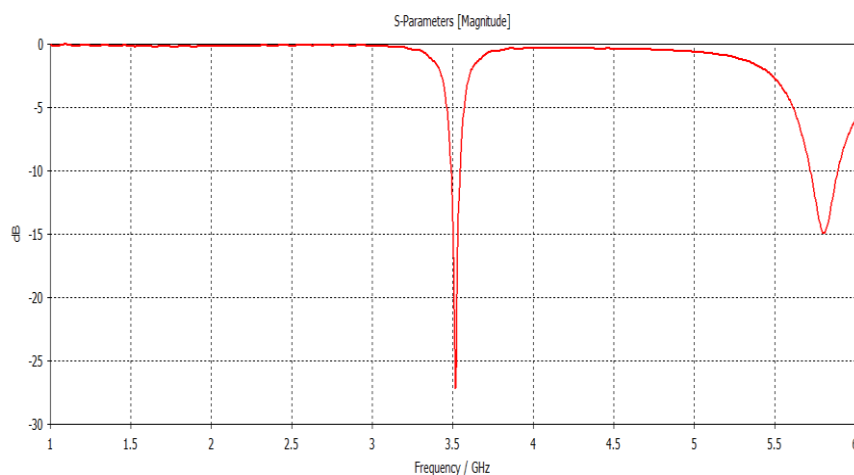


Fig. 5: Return loss of 3.5 GHz RMSA

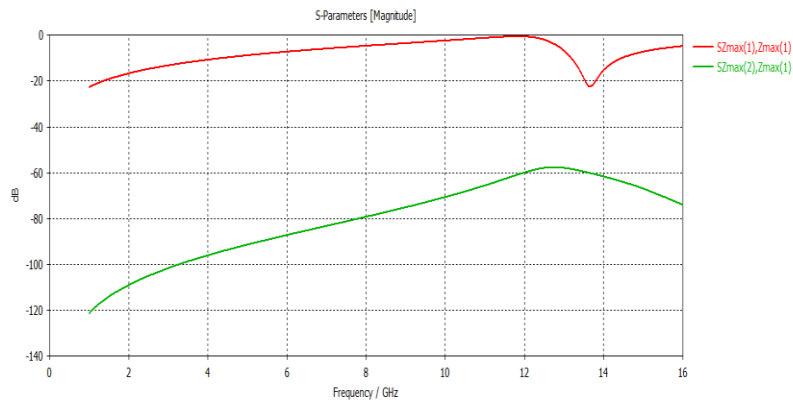


Fig. 6: S_{11} and S_{12} plot of SRR structure

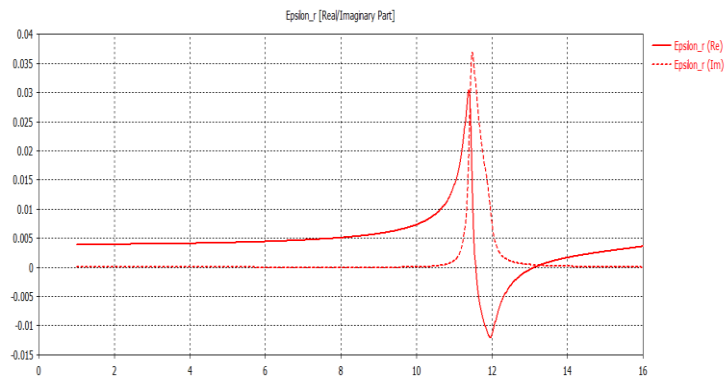


Fig. 7: Real and Imaginary values of permittivity

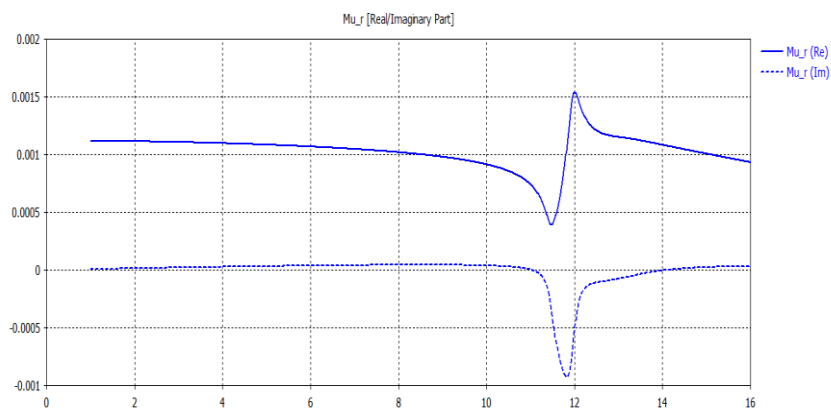


Fig. 8: Real and Imaginary values of permeability

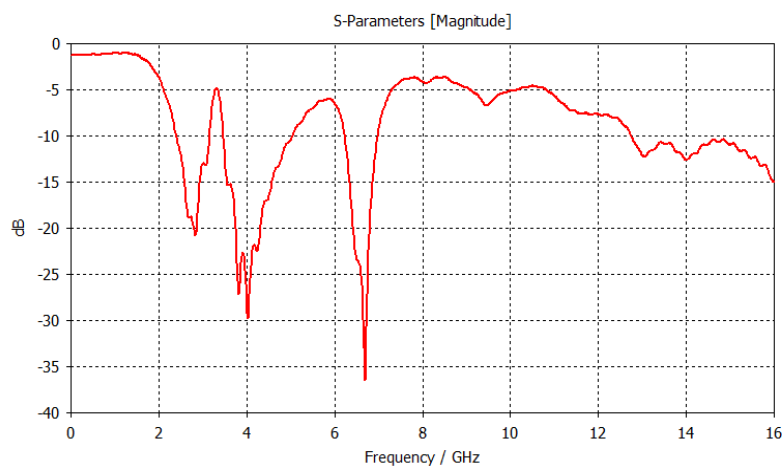


Fig. 9: Return loss of proposed 5G antenna

Using expressions from [14], the fractional percentage bandwidth of the designed antennas were calculated thus;

3.5 GHz single band patch antenna bandwidth:

$$= \frac{3.55-3.48}{3.5} \times 100\% = 2.00\%$$

Proposed patch antenna bandwidth at 2.4 GHz:

$$= \frac{3.18-2.36}{2.4} \times 100\% = 34.17\%$$

Proposed patch antenna bandwidth 3.5 GHz:

$$= \frac{5.07-3.46}{3.5} \times 100\% = 46.00\%$$

Proposed patch antenna bandwidth 5 GHz:

$$= \frac{7.02-6.22}{5} \times 100\% = 16.00\%$$

The proposed metamaterial-based rectangular microstrip antenna was also compared with some previously reviewed published journals along with other similar metamaterial antenna. Sharma *et al.* [7] reported that their antenna achieved impedance bandwidth of 10.6, 4.67, and 26.8% centred at 2.4, 3, and 5.7 GHz compared to 34.17, 46 and 16% at 2.4, 3.5 and 5 GHz achieved by the proposed metamaterial antenna, other comparisons are presented in Table III. From Table III, it is evident that all the reviewed works performed well but none matched the performance of the suggested metamaterial-based antenna in terms of bandwidth. Sizes of the different antennas would have been used as a yardstick for comparison only if they were all operating at the same frequency. It is equally important to note that the bandwidth considered is the combined impedance bandwidth across designed resonance frequencies.

Table 3: Comparison of suggested MTM-based antenna with some selected published works

| Antenna | f_r (GHz) | Bandwidth (MHz) |
|-------------------|-------------|-----------------|
| [7] | 2.4/3/5.7 | 42.07% |
| [10] | 2.4/3.5/5.6 | 264 |
| [20] | 1.8/3.1/5.8 | 700 |
| [21] | 3.8/5.3/8 | 1,050 |
| Proposed 2x2 RMSA | 2.4/3.5/6 | 3,500 |

V. CONCLUSION

A compact rectangular metamaterial-based microstrip antenna with triple band frequency (2.4/3.5/6 GHz) characteristics for fifth generation (5G) of mobile communication application along with Wireless Fidelity (WiFi) applications has been proposed in this study. The antenna consists of top rectangular patch with inscribed unit cell metamaterial, substrate and defected ground structure (DFS). The top rectangular patch bounded by two-unit cell of Square CSRR along the path adjoining the feedline was designed on an FR-4 epoxy substrate with dielectric constant (ϵ_r) of 4.2, thickness (h) of 1.6 mm and confined by DFG with designed dimensions of 30×10 mm to further enhance the miniaturization of the proposed antenna. Overall dimensions of the substrate after optimization on CST Studio was $30 \times 30 \times 1.6$ mm. The antenna achieved a combined bandwidth of 8.66 GHz, indicating a 50% fractional frequency, which, along with its compact form, makes the antenna suitable for handheld devices. Also, the proposed antenna showed great potentials for other satellite applications at frequencies beyond 10 GHz.

REFERENCES

- [1]. C. Duffy, "5G explained: What it is, who has 5G, and how much faster is it really?," *CNN Business*, 2020.
- [2]. Sarah Yost, "5G—It's Not Here Yet, But Closer Than You Think," *Electronic Design*, 2017.
- [3]. J. Horwitz, "The definitive guide to 5G low, mid, and high band speeds," *VentureBeat*, 2019.
- [4]. D. Burstein, "5G NR Only 25% to 50% Faster, Not Truly a New Generation," *2018-04-29*, 2018.
- [5]. S. Khangarot *et al.*, "A compact wideband antenna with detailed time domain analysis for wireless applications," *Ain Shams Eng. J.*, vol. 11, no. 4, pp. 1131–1138, Dec. 2020, doi: 10.1016/J.ASEJ.2020.02.008.
- [6]. U. M. Lambert, U. K. Michael, and O. A. Bernard, "Ultra-wideband Metamaterial-based Rectangular Microstrip Antenna for Sub-6 GHz 5G and other Microwave Applications," *J. Eng. Res. Reports*, vol. 25, no. 7, pp. 1–10, 2023, doi: 10.9734/jerr/2023/v25i7932.
- [7]. S. K. Sharma, J. D. Mulchandani, D. Gupta, and R. K. Chaudhary, "Triple-band metamaterial-inspired antenna using FDTD technique for WLAN/WiMAX applications," *Int. J. RF Microw. Comput. Eng.*, vol. 25, no. 8, pp. 688–695, Oct. 2015, doi: 10.1002/MMCE.20907.
- [8]. H. K. I. Ehab, "Design and Implementation of Dual-Band Microstrip Antennas for RFID Reader Application," *Ciencia E Tec. Vitivinic.*, no. September 2014, pp. 1–10, 2015.
- [9]. S. S. Rani and K. K. Naik, "Design and Analysis of Complimentary Split Ring Resonator with Slot on Retangular Patch Antenna for Wireless Applications," *Int. J. Recent Technol. Eng.*, vol. 7, no. 6, pp. 50–53, 2019.
- [10]. E. K. I. Hamad, W. A. E. Ali, M. Z. M. Hamdalla, and M. A. Bassiuny, "High gain triple band microstrip antenna based on metamaterial super lens for wireless communication applications," *Proc. 2018 Int. Conf. Innov. Trends Comput. Eng. ITCE 2018*, vol. 2018-March, pp. 197–204, Mar. 2018, doi: 10.1109/ITCE.2018.8316624.

- [11]. Y. Wang, N. Wang, T. A. Denidni, Q. Zeng, and G. Wei, "Integrated ultrawideband/narrowband rectangular dielectric resonator antenna for cognitive radio," *IEEE Antennas Wirel. Propag. Lett.*, vol. 13, pp. 694–697, 2014, doi: 10.1109/LAWP.2014.2314480.
- [12]. D. Thanuj, K. N. Saravana, N. B. Gnanamoorthi, and R. J. Stanislaus, "Metamaterial based compact planar antenna for UWB and 5G applications," *Proc. - 2nd Int. Conf. Micro-Electronics Telecommun. Eng. ICMETE 2018*, pp. 33–35, 2018, doi: 10.1109/ICMETE.2018.00020.
- [13]. R. K. Saraswat, "Design and Analysis of Metamaterial Inspired Multiband Antenna for 5G Sub-Six GHz NR Frequency Bands and wireless applications," pp. 1–29, 2022.
- [14]. C. A. Balanis, *Antenna Theory, Analysis and Design.*, 3rd ed. New Jersey: John Wiley & Sons, 2016.
- [15]. J. C. Saturday, K. M. Udofi, and A. B. Obot, "Compact Rectangular Slot Patch Antenna for Dual Frequency Operation Using Inset Feed Technique," *Int. J. Inf. Commun. Sci.*, vol. 1, no. 3, pp. 47–53, 2017, doi: 10.11648/j.ijics.20160103.13.
- [16]. A. B. Obot, G. A. Igwue, and K. M. Udofia, "Design and Simulation of Rectangular Microstrip Antenna Arrays for Improved Gain Performance," *Int. J. Networks Commun.*, vol. 9, no. 2, pp. 73–81, 2019, doi: 10.5923/j.ijnc.20190902.02.
- [17]. N. Abdullah, G. Bhardwaj, and Sunita, "Design of squared shape SRR metamaterial by using rectangular microstrip patch antenna at 2.85 GHz," *2017 4th Int. Conf. Signal Process. Integr. Networks, SPIN 2017*, pp. 196–200, 2017, doi: 10.1109/SPIN.2017.8049943.
- [18]. Rajni and A. Marwaha, "An accurate approach of mathematical modeling of SRR and SR for metamaterials," *J. Eng. Sci. Technol. Rev.*, vol. 9, no. 6, pp. 82–86, 2016, doi: 10.25103/jestr.096.11.
- [19]. H. R. Vani, Paramesha, and M. A. Goutham, "Design and Analysis Of Square Split Ring Resonator Metamaterial," *Int. J. Adv. Res. Eng. Technol.*, vol. 9, no. 6, pp. 196–201, 2018.
- [20]. C. Zhu, Z. Su, X. Dang, H. Zhai, L. Li, and C. Liang, "A CPW-Fed Triple Band Metamaterial Antenna with TER and CTER Loading," *IEEE Antennas Propag. Lett.*, vol. 1, pp. 3–6, 2014.
- [21]. T. Saeidi *et al.*, "High Gain Triple-Band Metamaterial-Based Antipodal Vivaldi MIMO Antenna for 5G Communications," *Micromachines 2021, Vol. 12, Page 250*, vol. 12, no. 3, p. 250, Feb. 2021, doi: 10.3390/MI12030250.